Eur. Phys. J. D **20**, 71–76 (2002)
DOI: 10.1140/epjd/e2002-00101-8

THE EUROPEAN PHYSICAL JOURNAL D

Control of bond-selective photochemistry in CH_2BrCl using adaptive femtosecond pulse shaping

N.H. Damrauer[1], C. Dietl[1], G. Krampert[1], S.-H. Lee[1,2], K.-H. Jung[2], and G. Gerber[1,a]

[1] Physikalisches Institut, Universität Würzburg, Am Hubland, 97074 Würzburg, Germany
[2] Department of Chemistry and School of Molecular Science (BK21), Korea Advanced Institute of Science and Technology, Taeduck Science Town, Taejon 305-701, Korea

Received 21 December 2001 / Received in final form 2 April 2002
Published online 28 June 2002 –

Abstract. Adaptive femtosecond laser pulse shaping is employed to achieve bond selective photodissociation/photoionization of CH_2ClBr in the gas phase. The photoproduct signal measured in a reflectron time-of-flight mass spectrometer is used as feedback to improve iteratively the spectral phases of the laser pulse *via* an evolutionary algorithm. We observe an increase of the fission of the stronger *versus* the weaker carbon halogen bond by 100%. Single parameter control schemes proved unable to achieve bond-selectivity. The complexity of the control problem is addressed by mapping it onto the well-known problem of maximizing second-harmonic generation (SHG). Further spectroscopic results indicate that the control involves manipulation of wave-packet dynamics on the neutral surfaces.

PACS. 82.50.Nd Control of photochemical reactions – 82.53.-k Femtochemistry

1 Introduction

The idea that the coherent properties of light might be used as tools for selectively cleaving particular bonds in polyatomic molecules has recently received much attention. An early approach to this problem has involved wavelength tuning of narrow-band UV laser sources to excite electronic transitions to the dissociative continua of selective bonds. In this context, polyhaloalkanes (*e.g.* CH_2XY) have served as model systems because of electronic transitions in halogen atoms in which a non-bonding electron is promoted to a carbon-halogen antibonding orbital (n(X)$\rightarrow\sigma^*$(C–X) or n(Y)$\rightarrow\sigma^*$(C–Y)). Successful application of this type of control has been demonstrated in the seminal work of Butler *et al.* on photoproduct distributions of gas-phase CH_2BrI [1]. In that work the excitation of the n(Br)$\rightarrow\sigma^*$(C–Br) transition at 210 nm resulted in exclusive fission of the stronger carbon-halogen (C–Br) bond while excitation to the red at 248 nm resulted in photoproduct distributions dominated by cleavage of the weaker C–I bond. While these studies were promising for wavelength control, the highly bond selective photochemistry observed for CH_2BrI makes it an interesting system for theoretical studies of coherent control [2]. Nevertheless this high selectivity is not a general condition found in all polyhaloalkanes. In studies of CH_2BrCl with nanosecond laser radiation, excitation (248 nm, 234 nm and 268 nm [3–5]) results in exclusive dissociation (as expected) along the weaker carbon-bromine bond. However excitation at 193 nm activates the cleavage of the stronger carbon-chlorine bond [3]. In contrast to CH_2BrI, cleavage of the weaker carbon-bromine bond still dominates the photochemistry at 193 nm. Such findings are also observed in studies of CF_2BrCl [6,7] as well as $CBrCl_3$ [8–10]. These experimental results can be understood in the context of theoretical work on CH_2XY model systems [11] which shows that the loss of photoproduct specificity following excited state evolution (initiated with higher photon energy excitation) is a result of strong non-adiabatic coupling among competing dissociation channels.

The question that arises is how can bond-selective photochemistry be achieved in systems with highly coupled competing dissociation channels? A novel approach to achieve such selectivity is the use of coherent light sources to actively manipulate the outcome of light/matter interactions by exploiting interference phenomena in both the time and frequency domain [12–16]. Specifically, we have applied femtosecond adaptive pulse shaping. This technique has been used to study a number of molecular systems in recent years [17–22]. The experiment reported here, however, is among the first to address bond selective photochemistry. That is to say, the bond broken in one channel is in any event preserved in the competing channel. The experiment reported here attempts to do just that using the model system CH_2BrCl.

2 Experimental

The femtosecond laser system used in this experiment delivers pulses with a duration of 80 fs, a pulse energy of 1 mJ

[a] e-mail: gerber@physik.uni-wuerzburg.de

at a center wavelength of 800 nm and at 1 kHz repetition rate. Modulation of the femtosecond spectral/temporal laser pulse profile is achieved with frequency-domain pulse shaping [23]. Details of our pulse shaper have been previously published [24]. Briefly, the device consists of a zero-dispersion compressor in a 4f-geometry, which is used to spatially disperse and recollimate the femtosecond laser pulse spectrum. A liquid-crystal display (LCD) placed in the Fourier plane of the compressor is the active element in the pulse shaping process. By applying different voltages to the 128 separate pixels the refractive indices across the laser spectrum can be changed. Upon transmission of the laser beam through the LCD, a frequency-dependent phase is acquired due to the individual pixel voltage values. In the control experiments described below, the spectral amplitudes have not been changed, and therefore the integrated pulse energy remains constant for different pulse shapes. In general control experiments, the optimal pulse to achieve a specific goal is not known in advance. Since the variational space of possible pulse shapes is so huge, scanning the complete parameter space is impossible. Following a suggestion by Judson and Rabitz [25], we therefore implement an iterative learning loop to search for optimized electric fields. At each iteration, the experimental outcome is evaluated with respect to the optimization goal determined by the experimenter at the outset. The global search method used for this purpose is an evolutionary algorithm [26,27]. Our implementation has been described in detail elsewhere [28].

The phase shaped femtosecond laser pulses are focused in an effusive molecular beam of the target molecules. This beam is prepared by expanding a room temperature liquid CH_2BrCl sample through a 60 μm nozzle at approximately 5 cm from the interaction region. CH_2BrCl was purchased from Merck Eurolab and used without further purification. The interaction of the shaped laser pulse with the parent molecules in the molecular beam, leads to different ionization and fragmentation processes. Cation mass spectra of the products are taken with a reflectron time-of-flight mass spectrometer (RETOF). Further details of the experimental setup have been described previously [29]. The laser pulse energy in the optimization experiments is about 230 μJ. This corresponds to a intensity of approximately 5×10^{13} W/cm^2 in the focus of the laser. Simultaneously, for each laser pulse the SHG yield is recorded with a 100 μm BBO crystal using a small laser beam pick-off. Optimizations are run either on optimizing (*i.e.* maximizing) the ratio of the signals of two ionic fragments or on maximizing SHG. As shown in earlier experiments, maximizing SHG leads to a bandwidth limited laser pulse [24,28].

3 Results and discussion

Previous demonstrations of photodissociation control using femtosecond adaptive pulse shaping in our group have relied on ionic mass fragment detection for implementation of feedback [18,30,31]. The mass spectrum obtained for CH_2BrCl following multi-photon excitation using intense (*ca.* 230 μJ/pulse), bandwidth-limited 800 nm laser pulses is shown in Figure 1a, normalized to the height of the $CH_2{}^{35}Cl^+$ fragment. The mass spectra (Figs. 1a and 1b) show two major fragment ions corresponding to the loss of bromine in the dominant feature (CH_2Cl^+) and loss of chlorine in the next prominent feature (CH_2Br^+). In both cases the expected isotope pattern due to presence of the halogen is observed. In Figure 1b we resolve in the vicinity of these ions small peaks one and two mass units lighter corresponding to CHX^+ and CX^+, respectively (X = Cl, Br). Also seen in a blown up spectrum (not shown) are minor contributions from CH_2^+, CH^+, and the parent molecular ion CH_2BrCl^+. A closer look at the baseline reveals Cl^+ and Br^+ peaks, approximately 20% of the parent ion signal (shown in the insets).

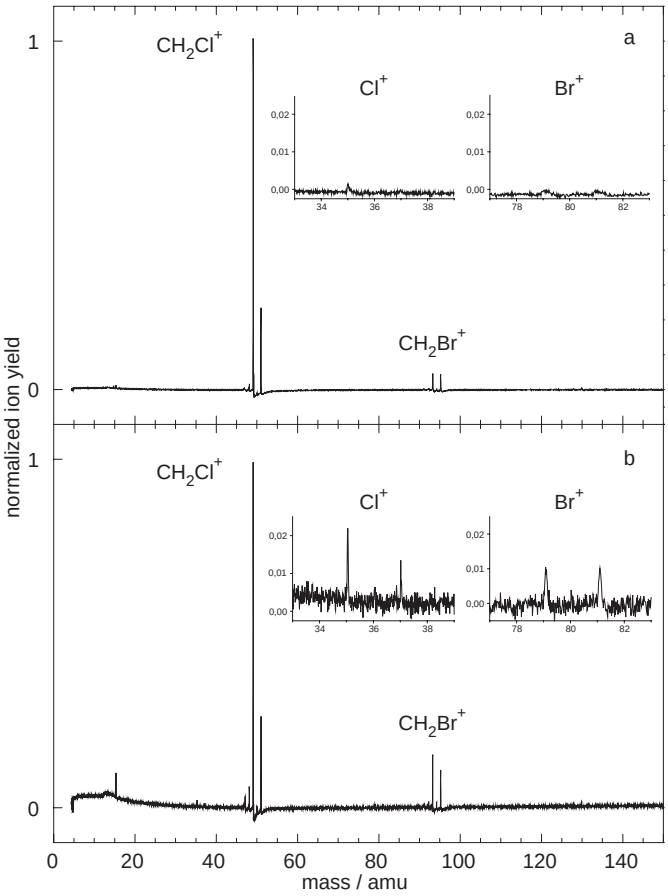

Fig. 1. Time-of-flight mass spectrum obtained for CH_2BrCl following multi-photon excitation with (a) a 80 fs bandwidth-limited 800 nm laser pulse ($\sim$ 230 μJ/pulse); (b) a phase shaped laser pulse found as the fittest individual of the last generation following maximization of the CH_2Br^+:CH_2Cl^+ ion ratio. The absolute yields are such that the CH_2Cl^+ fragment yield in (b) is about 6 times smaller than in (a). The insets in the plots show the signal of $^{35/37}Cl^+$, and $^{79/81}Br^+$, respectively, magnified by a factor of 40.

Focusing on the fragments CH_2Cl^+ and CH_2Br^+, resulting from carbon-halogen cleavage, we may ask whether phase shaped laser pulses can be used to optimize the

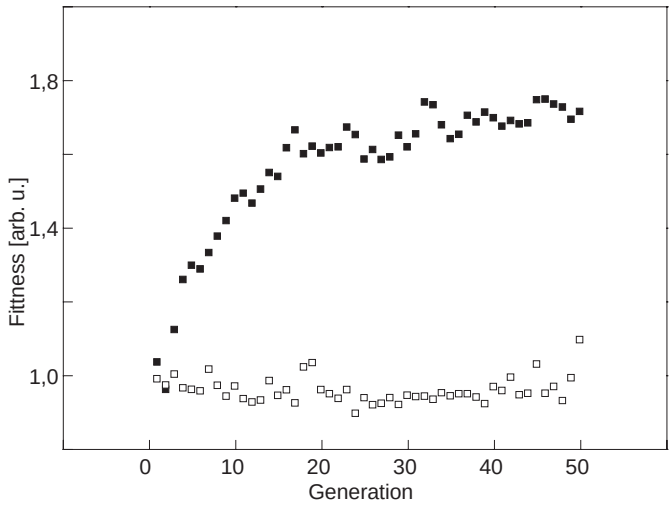

Fig. 2. Evolution curves measured for the optimization goal of maximization (filled squares) of the ion ratio CH_2Br^+/CH_2Cl^+. The values of the fittest individual per generation are plotted. Also shown (open squares) is the value of the ratio measured with an unmodulated (intense) laser pulse throughout the optimization process.

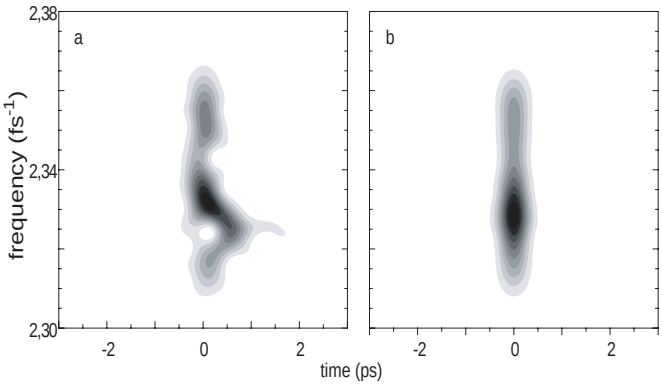

Fig. 3. Electric field shapes in Husimi representation for optimized pulses: (a) maximization of CH_2Br^+:CH_2Cl^+ ion ratio; (b) maximization of second harmonic generation. Black indicates regions of highest intensity and white of lowest intensity.

relative yield of these two reaction channels, *i.e.* maximizing the ratio of the two fragments. Thus we implemented adaptive femtosecond control using the signals arising from the single isotopic fragments $CH_2{}^{35}Cl^+$ and $CH_2{}^{79}Br^+$ as a feedback for the evolutionary algorithm. Optimizations were run with the goal of maximizing as well as minimizing the ratio CH_2Br^+/CH_2Cl^+. A threshold value was applied to the denominator to avoid unreasonably large and physically meaningless results if the denominator reaches values near the noise level. Although we report here data from one set of optimizations, we were able to repeat the experiments on three separate occasions and obtained similar results each time. The evolution curve for the maximization of CH_2Br^+/CH_2Cl^+ is shown in Figure 2 along with the value of the ratio measured with an unmodulated laser pulse throughout the optimization procedure. For the goal of maximization a strong increase of the ratio is seen compared to the value obtained with an unmodulated laser pulse. For the minimization case results are less convincing mainly because the algorithm explored areas in the parameter space that have an ion yield close to the noise level. Finally the algorithm found a less intense laser pulse and the ratio obtained from this is close to that found by energy attenuation of an unmodulated laser pulse (see below in the text). In the following we therefore concentrate on the maximization optimization.

Figure 1b shows the mass spectrum obtained with the best laser pulse of the last generation of the maximization experiment. The value of the ion ratio CH_2Br^+/CH_2Cl^+ was determined by integrating over the peak areas of the $CH_2{}^{79}Br^+$ and $CH_2{}^{35}Cl^+$ fragment signals. Following maximization, a value of 1:6 (CH_2Br^+/CH_2Cl^+) is achieved while a bandwidth-limited reference pulse yields a ratio of 1:12. These data show the ability to manipulate the ratio CH_2Br^+/CH_2Cl^+ by a significant amount using the optimization procedure. However, CH_2Cl^+ which results from the cleavage of the weaker bond still remains the major feature in all spectra for all the optimization goals chosen. The best pulse of the optimization produces a much larger amount of the corresponding smaller fragments Br^+ respectively Cl^+ than a bandwidth limited laser pulse. The signal arising from the cleavage of the stronger bond, Cl^+, is however larger than that from the cleavage of the weaker bond, Br^+.

In order to identify the control mechanism and to distinguish the adaptive phase shaping from simple pulse energy or pulse duration effects we take a closer look at the additional data taken during the optimizations. We first analyze the electric fields found for each optimization goal. Figure 3 shows the electric fields for the best laser pulses found in the last generation of each optimization using the Husimi representation. For the calculations, we have used the phase $\Phi(\omega)$ determined following maximization of SHG as a measure of the input phase of the pulses entering the pulse shaper. This is then subtracted from the phase measured at the pulse shaper (determined by the pixel voltages) for the result of the ratio maximization. These pulse shapes are in agreement with directly measured laser pulses using spectral interferometry. The Husimi plots clearly indicate a complex phase structure of the best laser pulse for the goal of maximizing (a) the ion ratio CH_2Br^+/CH_2Cl^+ in contrast to the flat phase laser pulse maximizing SHG (b).

The complex phase structure observed for the maximization of the ratio is a good indication that the particular phase shape of the pulses – and not just simple laser intensity reduction by increasing the pulse duration – is responsible for the obtained selectivity. To test this further, we map the unknown quantum control problem onto the well known problem of maximizing SHG [31]. In Figure 4, we show the value of the ratio CH_2Br^+/CH_2Cl^+ *versus* the measured SHG efficiency for each laser pulse explored during both optimizations: maximization of CH_2Br^+/CH_2Cl^+ (Fig. 4a) and maximization of SHG (Fig. 4b). When maximization of SHG is the goal, a set of randomly phase shaped laser pulses is the starting

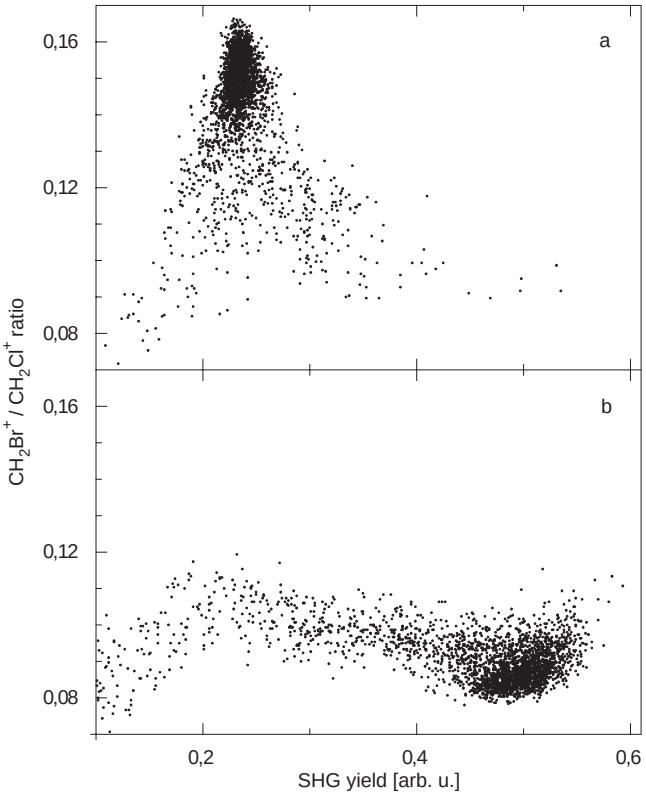

Fig. 4. Correlation diagram of CH_2Br^+:CH_2Cl^+ ion ratio *versus* measured SHG for all laser pulses explored in the two optimizations: CH_2Br^+:CH_2Cl^+ maximization (a), SHG maximization (b).

point for the evolutionary algorithm. The signal evolves during the optimization to higher intensities resulting in the shortest possible pulse. This evolution, thus, samples a wide variation in laser pulse intensity at constant laser pulse energy. It is seen that the ratio CH_2Br^+/CH_2Cl^+ changes only slightly during this intensity variation (we ignore ratio values below SHG = 0.1 which are subjected to a high degree of noise because there is no appreciable ion signal). The optimization of the CH_2Br^+/CH_2Cl^+ ratio shows a completely different behavior. Although the algorithm samples mainly laser pulses within in a narrow range of intensity it obtains a wide range in product ratios. Thus, the quantum control problem of maximizing the ratio of CH_2Br^+/CH_2Cl^+ cannot be solved with simple intensity variation like SHG maximization.

Besides increasing the pulse duration, the laser intensity can also be varied by attenuating the pulse energy while laser pulses remain temporally short. We therefore collected a series of mass spectra at different laser pulse energies. The product ratio of CH_2Br^+/CH_2Cl^+ obtained varies from 1:12 at 230 μJ to 1:13 at lower pulse energies. However, the determination of the ratio is problematic at low pulse energies due to the low ion count rates. The same problem is encountered in the minimization optimization, which yields a similar ratio. The low product ion count rates close to the noise level don't allow to draw any further conclusions about differences between energy attenuation and the minimization case. Nevertheless it is clear from these data that the ratio of 1:6 obtained in the maximization of CH_2Br^+/CH_2Cl^+ cannot be obtained with intensity variation by energy attenuation alone. These two experiments show that simple one parameter control schemes involving only intensity variations are not sufficient to achieve control in CH_2BrCl.

In addition to the above discussion several other interesting features are observed in the mass spectra. First, the fragmentation dynamics in the cases of SHG maximization and attenuation series do not appear to be significantly altered by the different laser pulse intensities. The mass spectrum collected following maximization of CH_2Br^+/CH_2Cl^+ in Figure 1b, on the other hand, shows substantial qualitative differences. Aside from a clear increase in the ratio of interest, the optimized pulse enhances not only the formation of smaller fragments such as CH_2^+, Cl^+, and Br^+, but at the same time formation of the parent ion. These features are a good indication that the laser pulse optimized for this task is in fact manipulating the fragmentation dynamics taking place. It is worth noting one additional feature observed in the spectrum of Figure 1b. The $CH_2{}^{79}Br^+$ peak used in the optimization goal is significantly enhanced with respect to its isotopic counterpart $CH_2{}^{81}Br^+$ which was not included in the optimization goal. These data suggest that complex phase shaped laser pulses are able to manipulate dissociation dynamics in extremely subtle ways. Femtosecond adaptive pulse shaping experiments to control isotope ratios in such halogenated systems are currently underway in our laboratory.

The optimization results presented here have shown that phase-shaped laser pulses found by the adaptive algorithm are able to maximize the ion ratio CH_2Br^+/CH_2Cl^+ compared with the ratio obtained using a bandwidth-limited 800 nm laser pulse. The question that arises is what is the nature of the dynamics that are subjected to control in this system? Unfortunately there is no simple answer to this question as there are multiple mechanisms by which CH_2Br^+ and CH_2Cl^+ photoproducts can be formed following multi-photon excitation of CH_2BrCl. For example, fragments can be created on neutral potential surfaces (and subsequently ionized for detection), *via* ion-pair surfaces, or *via* dissociative ionic surfaces. In order to address possible control pathways, we first reconsider the formation of photofragments when bandwidth-limited laser pulses are used. As was seen in Figure 1a, the shortest possible laser pulse ($\approx$ 80 fs; 230 μJ) gave rise to the two primary photoproducts CH_2Cl^+ and CH_2Br^+. In Figure 5a, two spectra are shown which were taken using nearly bandwidth-limited pulses of the different energies (360 μJ/pulse and 80 μJ/pulse). It is seen that over the more than four-fold change in pulse intensity (resulting in a strong decrease of total ion signal), the spectra remain qualitatively similar without any significant intensity of the parent ion. It is emphasized that at all pulse energies explored the parent ion does not appear in the spectrum with significant relative intensity. Spectra collected using 400 nm excitation, on the other hand, show a remarkable qualitative difference. In Figure 5b, mass spectra are

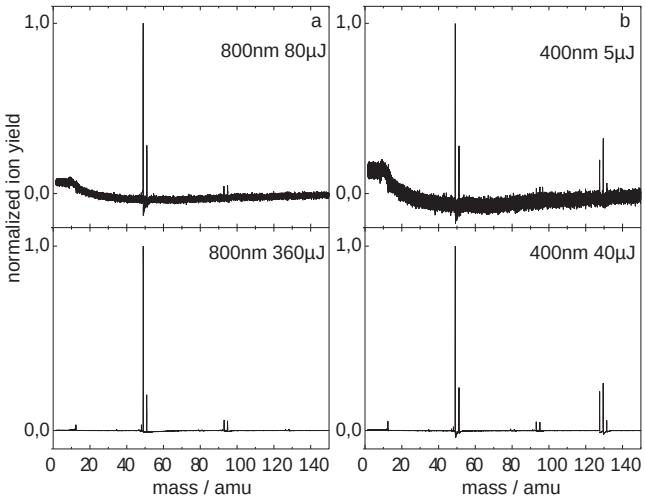

Fig. 5. Mass spectra obtained with 800 nm (a) and 400 nm (b) excitation. The laser pulse energy was and 80 μJ/pulse and 360 μJ/pulse for the 800 nm excitation (a) 5 μJ/pulse and 40 μJ/pulse for the 400 nm excitation (b).

presented again obtained at different laser pulse energies (40 μJ/pulse and 5 μJ/pulse) at 400 nm excitation wavelength. It is seen that the relative heights of the CH_2Cl^+ and CH_2Br^+ signals appear comparable to those collected using 800 nm excitation. However, when 400 nm excitation is used, the parent ion CH_2BrCl^+ is a major photoproduct in the mass spectrum and this is the case at all pulse intensities explored.

As already mentioned, there are multiple mechanisms by which CH_2Br^+ and CH_2Cl^+ photofragments can be formed following multi-photon 800 nm excitation of CH_2BrCl. Based on the observations shown in Figure 5, it is unlikely that the products form on dissociative ionic surfaces. First, if we consider the 400 nm spectra, the observation of the CH_2BrCl^+ parent ion peak shows that at least one bound ionic state is involved. Those states lie above the ionization threshold at 10.77 eV but below the dissociative ionic states. If the fragments CH_2Br^+ and CH_2Cl^+ arise from dissociative ionic surfaces, a strong laser intensity dependence in the relative yield of the parent ion to the fragment ions would be observed. In the mass spectra collected, however, the relative yield of parent ion to CH_2Cl^+ remains approximately constant as the laser intensity is increased considerably from 5 μJ/pulse to 40 μJ/pulse. Second, if we consider the mass spectra collected with 800 nm excitation, there is no significant contribution from the parent ion signal during the more than four-fold pulse intensity reduction. Since photoproduct formation *via* dissociative ionic surfaces of CH_2BrCl requires that more than eleven 800 nm photons (> 17 eV) be absorbed in about 100 fs it is unreasonable to expect that the relative ion yields would not change during this intensity reduction. This is especially true in light of the observation that the parent ion is so prominent in the 400 nm spectra at all intensities explored.

In the above discussion, dissociative ionization is ruled out as a major origin of CH_2Br^+ and CH_2Cl^+ ion formation. Therefore, the dynamics on neutral surfaces are mainly responsible for the molecular fragmentation. Of the possible mechanisms available to the CH_2BrCl system, the most promising is one in which an electron from a non-bonding lone pair of a halogen atom is initially excited to Rydberg states by the bandwidth-limited 800 nm laser pulse [32]. Such states can then be pre-dissociated by ion-pair states wherein a bonding electron is transferred from the alkyl-halide to the halogen atom that has undergone the Rydberg transition. This has been observed for related molecules such as CH_3Cl and CH_3Br [33,34]. It is emphasized that within this mechanism, one of the carbon-halogen bonds in CH_2BrCl is broken in a way which leads directly to the formation of an alkyl-halide cation (CH_2Cl^+ or CH_2Br^+) and the corresponding halogen anion (Br^- or Cl^-, respectively). Because we detect only cations in the TOF spectrometer, the CH_2Cl^+ and CH_2Br^+ fragments would dominate the mass spectrum. This is entirely consistent with our spectroscopic results using 800 nm excitation. It explains especially the low relative yield of Cl^+ and Br^+ fragments when bandwidth-limited laser pulses are used. The increase of the Cl^+ respectively Br^+ signal following optimization indicates that the control mechanism is less favorably using the ion-pair surfaces.

In the arguments presented above, a bandwidth-limited 800 nm laser pulse produces CH_2Br^+ and CH_2Cl^+ fragments preferentially *via* dynamics involving Rydberg states that are then predissociated by ion-pair states. This is an interesting situation because the phase-shaped pulses optimized for maximizing the CH_2Br^+/CH_2Cl^+ ratio have a complex temporal shape and are therefore significantly less intense. This implies that the surfaces on which control is taking place are likely to be lower in energy. As a result of this, it is entirely reasonable that control takes place because the shaped laser field is able to manipulate wave packet motion on the neutral σ^*(C–X) (X = Cl, Br) repulsive surfaces discussed in the introduction. It is noted that transitions to the σ^*(C–Br) and σ^*(C–Cl) surfaces take place at 6.04 eV and 7.55 eV, respectively, which can be easily accessed by absorption of four 800 nm photons (6.20 eV) or five 800 nm photons (7.75 eV). As spectroscopic evidence in support of a control mechanism using such surfaces, we first note the enhancement of the smaller mass fragments Br^+ and Cl^+ following the CH_2Br^+/CH_2Cl^+ maximization pulse (Fig. 1b). This is consistent with a mechanism wherein the neutral fragments formed on the repulsive surfaces are subsequently ionized by the temporally elongated phase-shaped pulse. In addition, we note the larger relative size of the Cl^+ signal with respect to the Br^+ signal. This suggests that the shaped excitation pulse uses the dissociative neutral surfaces, but does so in a way that enhances the breakage of the stronger C–Cl bond over breakage of the weaker C–Br bond leading to the maximization result. The continued prominence of CH_2Cl^+ over CH_2Br^+ (despite the reversed intensity of Br^+ and Cl^+ signals) would simply suggest that even with this optimized pulse, a substantial amount of the fragment ions continue to be formed *via* ion-pair states.

4 Conclusions

The results presented show that femtosecond adaptive pulse shaping is a powerful tool for manipulating photoproduct distributions. We have shown that shaped laser pulses can be found which both minimize and maximize the ion ratio CH_2Br^+/CH_2Cl^+ with respect to that achieved with a bandwidth-limited laser pulse. This is done automatically and without prior knowledge of the molecular potential energy surfaces involved. Concentrating on the maximization case, a complex laser pulse is discovered which more than doubles the ion ratio. We emphasize that this corresponds to a significant relative change in the breaking of the stronger carbon-halogen bond. Intensity dependence measurements show that this effect is not simply a result of intensity changes in the laser pulse. It appears rather that the shaped laser pulse changes the fragmentation dynamics and the control mechanism may involve manipulation of wave packet motion on neutral dissociative surfaces which are not involved in photoproduct formation when bandwidth-limited 800 nm pulses are used. These results are an encouraging indication that even in systems such as CH_2BrCl (where excited states are highly coupled), complex laser fields may be useful for achieving bond-selective photochemistry.

Financial support from the European Coherent Control Network (COCOMO): HPRN-CT-1999-00129, the German-Israeli Cooperation in Ultrafast Laser Technologies (GILCULT): FKZ-13N7966, and the "Fonds der chemischen Industrie" is gratefully acknowledged. N.H. Damrauer acknowledges financial support from the Alexander von Humboldt-Stiftung and S.-H. Lee from the Korea Science and Engineering Foundation and Deutscher Akademischer Austauschdienst.

References

1. L.J. Butler, E.J. Hintsa, S.F. Shane, Y.T. Lee, J. Chem. Phys. **86**, 2051 (1987)
2. D.G. Abrashkevich, M. Shapiro, P. Brumer, J. Chem. Phys. **116**, 5584 (2002)
3. W.B. Tzeng, Y.R. Lee, S.M. Lin, Chem. Phys. Lett. **227**, 467 (1994)
4. W.S. McGivern, R. Li, P. Zou, S.W. North, J. Chem. Phys. **111**, 5771 (1999)
5. S.H. Lee, Y.J. Jung, K.H. Jung, Chem. Phys. **260**, 143 (2000)
6. G. Baum, J.R. Huber, Chem. Phys. Lett. **213**, 427 (1993)
7. A. Yokoyama, K. Yokoyama, T. Takayanagi, J. Chem. Phys. **114**, 1617 (2001)
8. Y.J. Jung, M.S. Park, Y.S. Kim, K.H. Jung, H.R. Volpp, J. Chem. Phys. **111**, 4005 (1999)
9. Y.R. Lee, W.B. Tzeng, Y.J. Yang, Y.Y. Lin, S.M. Lin, Chem. Phys. Lett. **222**, 141 (1994)
10. Y.R. Lee, Y.J. Yang, Y.Y. Lin, S.M. Lin, J. Chem. Phys. **103**, 6966 (1995)
11. T. Takayanagi, A. Yokoyama, Bull. Chem. Soc. Jpn **68**, 2225 (1995)
12. S.A. Rice, M. Zhao, *Optical control of molecular dynamics* (Wiley, New York, 2000)
13. R.J. Gordon, S.A. Rice, Annu. Rev. Phys. Chem. **48**, 601 (1997)
14. H. Rabitz, W. Zhu, Acc. Chem. Res. **33**, 572 (2000) and references therein
15. M. Shapiro, P. Brumer, Adv. At. Mol. Opt. Phys. **42**, 287 (2000)
16. T. Brixner, N.D. Damrauer, G. Gerber, Adv. At. Mol. Opt. Phys. **46**, 1 (2001)
17. C.J. Bardeen, V.V. Yakovlev, K.R. Wilson, S.D. Carpenter, P.M. Weber, W.S. Warren, Chem. Phys. Lett. **280**, 151 (1997)
18. A. Assion, T. Baumert, M. Bergt, T. Brixner, B. Kiefer, V. Seyfried, M. Strehle, G. Gerber, Science **282**, 919 (1998)
19. T.C. Weinacht, J. White, P.H. Bucksbaum, J. Phys. Chem. A **103**, 10166 (1999)
20. T. Hornung, R. Meier, D. Zeidler, K.L. Kompa, D. Proch, M. Motzkus, Appl. Phys. B **71**, 277 (2000)
21. D. Meshulach, Y. Silberberg, Nature **396**, 239 (1998)
22. R.J. Levis, G.M. Menkir, H. Rabitz, Science **292**, 709 (2001)
23. A.M. Weiner, Rev. Sci. Instrum. **71**, 1929 (2000)
24. T. Brixner, M. Strehle, G. Gerber, Appl. Phys. B **68**, 281 (1999)
25. R.S. Judson, H. Rabitz, Phys. Rev. Lett. **68**, 1500 (1992)
26. D.E. Goldberg, *Genetic algorithms in search, optimization, and machine learning* (Addison-Wesley, Reading, 1993)
27. H.P. Schwefel, *Evolution and optimum seeking* (Wiley, New York, 1995)
28. T. Baumert, T. Brixner, V. Seyfried, M. Strehle, G. Gerber, Appl. Phys. B **65**, 779 (1997)
29. L. Bañares, T. Baumert, M. Bergt, B. Kiefer, G. Gerber, J. Chem. Phys. **108**, 5799 (1998)
30. M. Bergt, T. Brixner, B. Kiefer, S.M., G. Gerber, J. Phys. Chem. A **103**, 10381 (1999)
31. T. Brixner, B. Kiefer, G. Gerber, Chem. Phys. **267**, 241 (2001)
32. T. Ibuki, A. Hiraya, K. Shobatake, J. Chem. Phys. **96**, 8793 (1992)
33. S. Suzuke, K. Mitsuke, T. Imamura, I. Koyano, J. Chem. Phys. **96**, 7500 (1992)
34. K. Suto, Y. Sato, C.L. Reed, V. Skorokhodov, Y. Matsumi, M. Kawasaki, J. Phys. Chem. A **101**, 1222 (1997)